Journal of Solid State Chemistry 185 (2012) 95–100

Contents lists available at SciVerse ScienceDirect

Journal of Solid State Chemistry

journal homepage: www.elsevier.com/locate/jssc

Synthesis and characterization of nanoapatites organofunctionalized with aminotriphosphonate agents

Sanaâ Saoiabi [a,b,c], Sanae El Asri [a], Abdelaziz Laghzizil [a,*], Sylvie Masse [b], Jerome L. Ackerman [c,*]

[a] Laboratoire de Chimie Physique Générale, Faculté des Sciences BP 1014, Université Mohamed V-Agdal, Rabat, Morocco
[b] UPMC Univ Paris 06, UMR 7574, Chimie de la Matière Condensée de Paris, 4 Place Jussieu, F-75005 Paris, France
[c] Biomaterials Laboratory, Martinos Center for Biomedical Imaging, Department of Radiology, Massachusetts General Hospital and Harvard Medical School, Room 2320, 149 13 Street, Charlestown, MA 02129, USA

ARTICLE INFO

Article history:
Received 14 June 2011
Received in revised form
8 October 2011
Accepted 17 October 2011
Available online 26 October 2011

Keywords:
Apatite
Functionalized surface
Mesoporous materials
Surface properties

ABSTRACT

Organofunctionalized apatite nanoparticles were prepared using a one step process involving dissolution/precipitation of natural phosphate rock and covalent grafting of nitrilotris(methylene)triphosphonate (NTP). The synthesized materials were characterized by Brunauer–Emmett–Teller (BET) surface measurement, thermogravimetry, inductively coupled plasma emission spectroscopy (ICP–ES), elemental analysis, multinuclear solid state cross-polarization/magic angle spinning (CP/MAS) and single-pulse NMR spectroscopy, transmission electron microscopy (TEM) and energy dispersive X-ray analysis (EDXA). After grafting BET measurements yielded particle specific surface areas ranging from 88 to 193 $m^2\,g^{-1}$ depending on the grafted phosphonate. The results show that the surfaces of the nanoapatite particles can be covered with functional groups bound through a variable number of R–P–O–Ca bonds to render them organoapatites.

Published by Elsevier Inc.

1. Introduction

Apatites are orthophosphates exhibiting a rich, highly complex, often confusing chemistry, the term "apatite" being derived from the Greek $\alpha\pi\alpha\tau\alpha\omega$, meaning "fraud" or "deceive". Hydroxyapatite $Ca_{10}(PO_4)_6(OH)_2$ (HAp) is a naturally occurring mineral widely used in development of bioceramics, environmental sorbents and heterogeneous catalysis [1–6]. In terms of composition, the mineral resembles the nanocrystals embedded in the collagenous matrix in all vertebrate bone and in the dentin and enamel of teeth; the surface chemistry of bone nanocrystals has important implications for both bone biology and for the action of pharmaceuticals used to treat metabolic bone disease [7]. Thus, apatite interfacial chemistry and the derivatization of apatite nanocrystal surfaces have widespread relevance to many areas in chemistry, biology, materials science, geochemistry, environmental remediation and medicine.

In recent years, many studies have demonstrated that a wide range of additives, such as silane [8] and titanate-coupling agents [9,10], biomacromolecules [11] and polymers [12] can modify the structure and morphology of apatite and control its nucleation. Above all, a number of studies have been carried out to elucidate the effect of various organic molecules on the crystallization of hydroxyapatite. On the other hand, phosphonate additives have important applications in the biomineralization process [13], most importantly to control the remodeling of bone in the treatment of osteoporosis and other diseases of bone metabolism [14]. The usefulness of organophosphonates is enhanced by their stability over wide ranges of pH and temperature. Thus, several works were carried out on the preparation of hybrid apatites demonstrating the influence of small organic ligands on structural and thermal properties, knowing that the organic species are among the most effective inhibitors of the crystal growth of calcium phosphates [15]. Tanaka et al. [16] succeeded in grafting monohexylphosphate and monodecylphosphates. Other studies were devoted to the morphological control of apatite growth, for example, through a polymeric route using calcium nitrate and phenydichlorophosphine $C_6H_5PCl_2$ as starting materials enabling the formation of hydroxyapatite layers [17]. El Hammari et al. [18] prepared organohydroxyapatite products via a rapid precipitation method by reacting $Ca(OH)_2$ and $NH_4H_2PO_4$ in the presence of phenyl and alkyl phosphonate species separately. The latter results indicate that the phosphonate introduced into the apatite lattice has a strong effect on its specific surface area and porosity. In addition, Silva et al. [8] demonstrated that silylation of apatite by $(CH_3O)_3SiR$ agents affects the surface properties and therefore heavy metal adsorption by the presence of the amine function in the organic surface group. Colloidal synthesis and characterization of a crystalline apatite hybrid with aminoethylphosphate ligands have been achieved in Ref. [19],

* Corresponding authors. Fax: +1 617 726 7422.
E-mail addresses: laghzizi@fsr.ac.ma (A. Laghzizil), jerry@nmr.mgh.harvard.edu (J.L. Ackerman).

0022-4596/$ - see front matter Published by Elsevier Inc.
doi:10.1016/j.jssc.2011.10.031

demonstrating that ultrafine individualized calcium phosphate nanophosphors displaying amino groups on their surfaces are good candidates for use as fluorescent probes in biological imaging. However, the high reactivity of apatites with organic phosphorus molecules resides in the presence of charges and hydrogenous active sites on their surfaces, in particular the amphoteric sites ≡Ca–OH and ≡P–OH [20]. The presence of these hydrogenous sites enables reaction with organic additives to form hybrid apatites [21], whereas organic surface moieties can change the surface chemical (hydrophilicity, hydrophobicity, reactivity) properties of the solid, as well as structural and physical properties.

It is well known that nanoapatite powders can be produced using different methods such as sol–gel [22], hydrothermal [23] or precipitation methods [24,25], through a double decomposition reaction in aqueous solution between $Ca(NO_3)_2$ and $(NH_4)_2HPO_4$, or by a neutralization reaction in which $Ca(OH)_2$ is neutralized by H_3PO_4 in an aqueous slurry. Up to now, the precipitation route is often employed in industrial hydroxyapatite synthesis because of the availability of low cost raw materials, as well as its relative simplicity. There are several investigations on the preparation of nanosized apatites under optimal conditions, illuminating the influence of temperature, pH and the presence of surface modifiers on the size and phase composition of the obtained material [23–26].

In this work, hydrophobic hydroxyapatite particles with structural features in the range below 100 nm were synthesized *in situ* in aqueous solution in the presence of nitrilotris(methylene)triphosphonates (NTPs) using calcium and phosphorus precursors from Moroccan natural phosphate. The present investigation explores a novel synthesis and characterization of hybrid mesoporous apatite resulting from the simultaneous reactions of the dissolution of natural phosphate and the precipitation of mesoporous apatite in the presence of nitrilotris(methylene)triphosphonate (NTP) species. With a one-step grafting process, multifunctional molecules containing phosphonate and nitrogen groups with a reactive center are formed and linked to the apatite surface. In a companion paper, we describe a first environmental application using these new organo-structured mesoapatites for removal of lead from aqueous solution. The ability to modify an apatite surface with specific ligand fields creates powerful new capabilities for other applications such as catalysis, chemical separations and sensor development.

2. Experimental

2.1. Sedimentary phosphate rock

Phosphate rock samples used here come from an extracted ore of Bengurir (Morocco). Prior to use, this material requires initial treatments such as crushing and washing. The 100–400 μm grain size fraction was washed with distilled water several times to remove the soluble matter. As published elsewhere [27], the chemical composition of the natural phosphate was determined as: Ca (37.84%), P (15.03%), F (3.07%), Si (1.78%), S (0.78%), Na (0.79%) and other negligible elements. The structure and morphology of the phosphate rock sample was estimated using different characterization techniques. X-ray diffraction indicated the presence of two main inorganic components (apatite + quartz-SiO_2). Therefore, solid-state NMR spectroscopy was used to identify the environments of phosphorus, silicon and carbon in the Bengurir natural phosphate. Thermal analysis showed that small quantities (7 wt%) of organic components were still present [27].

2.2. Synthesis of grafting minerals

All chemicals of reagent quality were obtained from Aldrich Chemical Co (St. Louis, MO, USA). Nitrilotris(methylene)triphosphonic acid (Fig. 1) was used as a commercial 50 wt% solution in water. The preparation of grafted apatites followed the same process described in a previous study [28], except that the NTP phosphonate was introduced in (Ca+P) solution: a phosphate rock (PR) mass of 20.6 g was dissolved in 500 ml of deionized water adjusted to pH=2 with 1 M•HNO_3 solution and then stirred for 3 h. After dissolving, the solution was filtered and the filtrate was mixed under vigorous stirring with nitrilotris(methylene)triphosphonates (NTP) in varying proportions. The transparent mixture was precipitated using 20 mL of concentrated ammonia solution at pH=10. The final white suspensions were aged for 24 h at room temperature, filtered, washed with deionized water and then dried overnight at 100 °C. The sample labels (e.g., × % NTP) refer to the molar ratio organic phosphorus/(organic+inorganic phosphorus).

2.3. Techniques

The crystalline phases were identified using a Philips (Eindhoven, The Netherlands) PW131 powder X-ray diffractometer (XRD) using a copper source. Infrared spectra were recorded from 400 to 4000 cm^{-1} on a Bruker (Carlsruhe, Germany) IFS 66v Fourier transform spectrometer using KBr pellets. The N_2 adsorption–desorption isotherms for dried powders were obtained by multipoint N_2 gas sorption experiments at 77 K using a Micromeritics (Norcross, GA) ASAP 2010 instrument. The specific surface areas were calculated according to the Brunauer–Emmett–Teller (BET) method using adsorption data in the relative pressure range from 0.05 to 0.25, whereas the pore size and volume were estimated using the Barret–Joyner–Halenda (BJH) approximation. Thermogravimetry (TG) was carried out in flowing air using a TA Instruments (New Castle, DE) Netzsch STA-409 EP apparatus. Samples were initially dried at 100 °C. Thermal measurements were conducted from 30 to 1000 °C at a 10 °C/min heating rate. The sample powder was chemically analyzed by inductively coupled plasma (ICP) emission spectroscopy (Shimadzu ICPS-7500, Kyoto, Japan) and elementary CNHOS analyses. Solid-state ^{13}C and ^{31}P NMR spectra were obtained at frequencies of 75.5 and 121 MHz, respectively, using single 90° pulse magic angle spinning (MAS) measurements on a Bruker (Karlsruhe, Germany) 300 MHz spectrometer. Transmission electron microscopic (TEM) analysis with energy dispersive (EDXA) detection was performed on Cu-coated carbon grids using a high resolution thermal field emission electron microscope equipped with an EDXA system for elemental analysis (NEKAI-G^2 environmental transmission electron microscope) operating at 100 kV (Fig. 1).

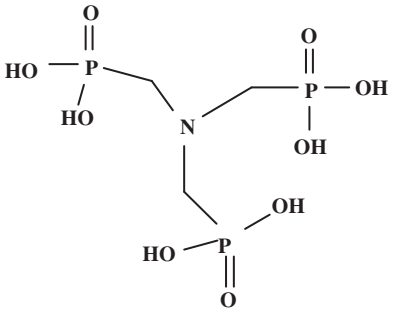

Fig. 1. Structure of nitrilotris(methylene)triphosphonic acid.

3. Results and discussion

3.1. Characterization of grafted apatite

XRD patterns of the as-prepared products showed a poorly crystalline apatite structure, the crystallinity of which strongly depended on the NTP concentration (Fig. 2). Powder x-ray diffraction revealed the presence of very small particles and a significant degree of disorder in the apatite lattice caused by the presence of NTP molecules, which inhibit apatite crystallization. The structural disorder induced by NTP incorporation is responsible for the observed reduction of the thermal stability of the grafted materials. In fact, heat treatment of the powders induces a partial conversion of NTP–HAp particles into β-tricalcium phosphate β-$Ca_3(PO_4)_2$ (β-TCP), the extent of this conversion increasing with the incorporated NTP content. However, for environmental applications, i.e., using the grafted products as adsorbents, no heat treatment is recommended to conserve the surface properties and the chemical composition of the materials.

Infrared spectra of the various products display the vibrational modes of PO_4 groups at 1100, 1050, 960, 605 and 564 cm^{-1} characteristic of the apatite structure (Fig. 3). The small displacement of PO_4 bands to high frequencies with NTP content is related to the structural disorder and the nature of the P–O bond [29]. However, the P–O bands from organic phosphorus PO_3^{2-} in NTP molecules overlap those of inorganic PO_4^{3-} ions in the apatite lattice. The FT-IR spectra of grafted NTP–HAp composites exhibit weak peaks originating from organic carbon in the wavenumber range of 1420–1450 cm^{-1}, contrary to the ungrafted materials, which are carbonated apatites. This reflects the replacement of CO_3^{2-} ions originally in the phosphate rock with phosphonate groups in the grafted materials. Strong carbonate bands are found in both the starting PR material and in the reference sample prepared without NTP species. After surface grafting, new

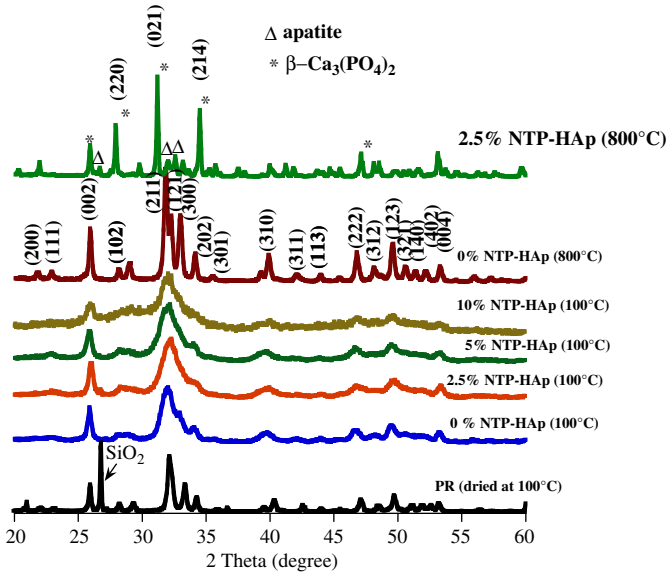

Fig. 2. Change in XRD patterns of NTP–HAP treated with various NTP agents as received and after heating, compared to that of the phosphate rock (PR) starting material.

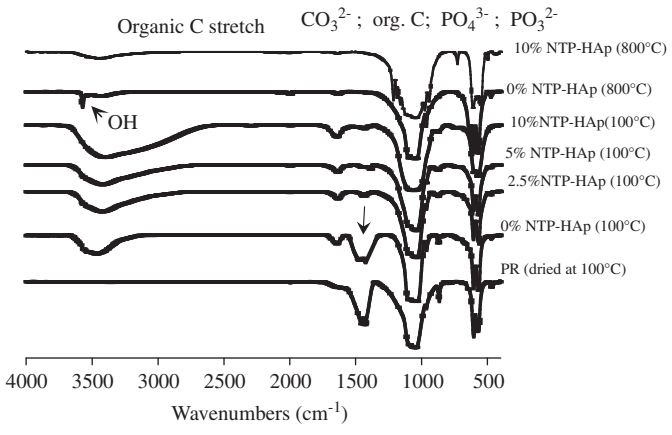

Fig. 3. FT-IR spectra of NTP–HAp powders with various NTP concentrations as-received and after heating at 800 °C, compared to that of the phosphate rock (PR) starting material.

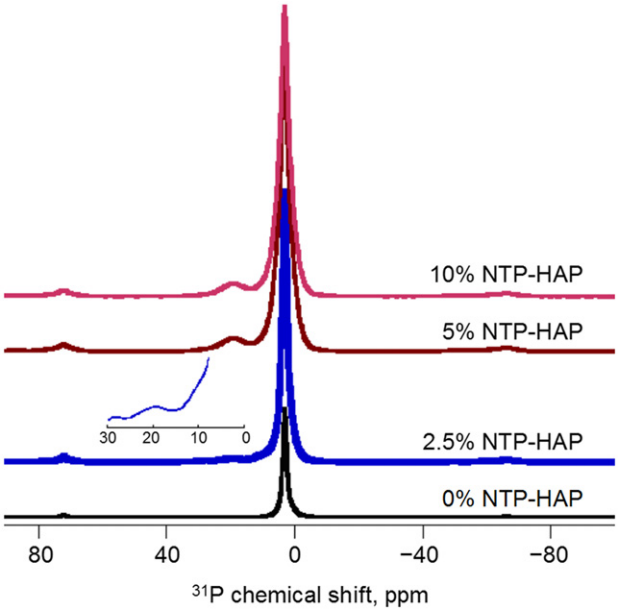

Fig. 4. ^{31}P NMR spectra of NTP-grafted HAp and pure HAp as reference (0% NTP). The peaks at ±70 ppm are rotational sidebands (artifacts resulting from the spinning and not actual resonances).

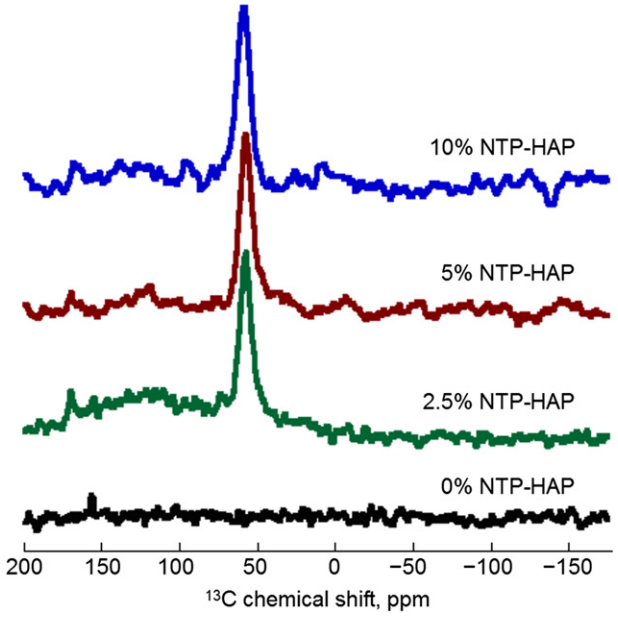

Fig. 5. ^{13}C NMR spectra of NTP-grafted HAp and pure HAp (0% NTP) as a reference.

Table 1
Chemical composition and porosity characteristics of pure and graft-modified apatites: elemental analysis, calcium/phosphorus molar ratio, thermogravimetric weight loss, specific surface area S_{BET}, specific pore volume V_p, mean pore diameter D_p and lead (II) adsorption capacity q_{max}.

Solid	%Ca	%P	%C	%N	Ca/P	Wt. loss % 200–600 °C	S_{BET} ($m^2\ g^{-1}$)	V_p ($cm^3\ g^{-1}$)	D_p (nm)	q_{max} (mmol g^{-1})
PR							20			0.48
0% NTP	38.66	15.33	0.30	–	1.95	2.02	150	36.2	11.5	1.68
2.5% NTP	34.31	16.24	0.52	0.20	1.61	3.49	193	45.2	9.5	2.13
5% NTP	34.41	17.10	0.72	0.32	1.55	4.62	148	35.5	25	2.97
10% NTP	34.39	17.39	1.05	0.62	1.53	6.03	145	33.3	38	3.06
20% NTP	34.01	17.05	1.65	–	1.52	7.10	88	20.2	40	–

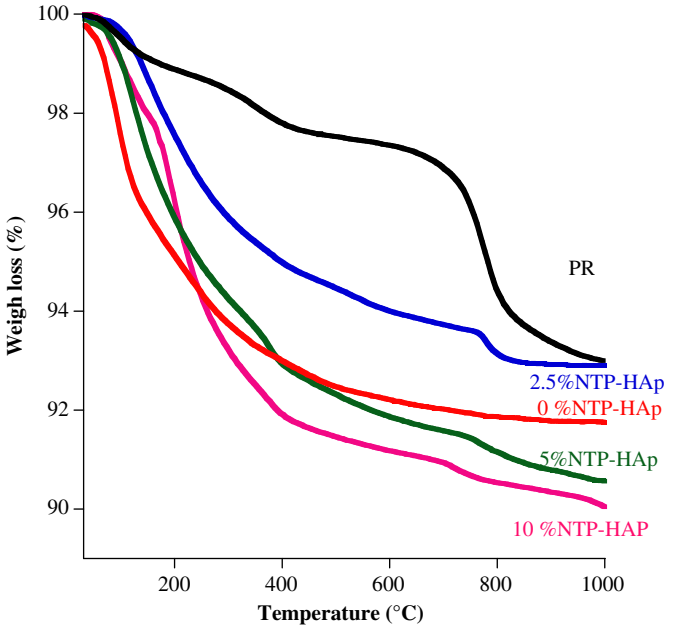

Fig. 6. TG analyses of pure and NTP-grafted apatites.

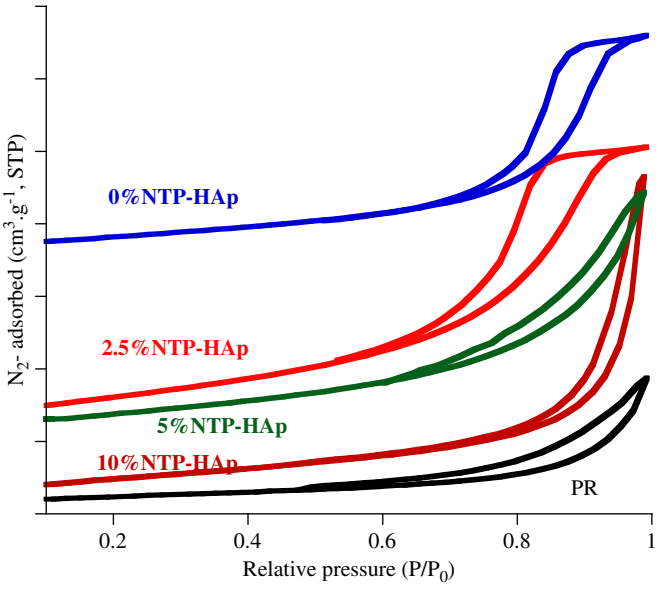

Fig. 8. N_2-sorption isotherms at 77 K of pure and NTP-grafted apatites.

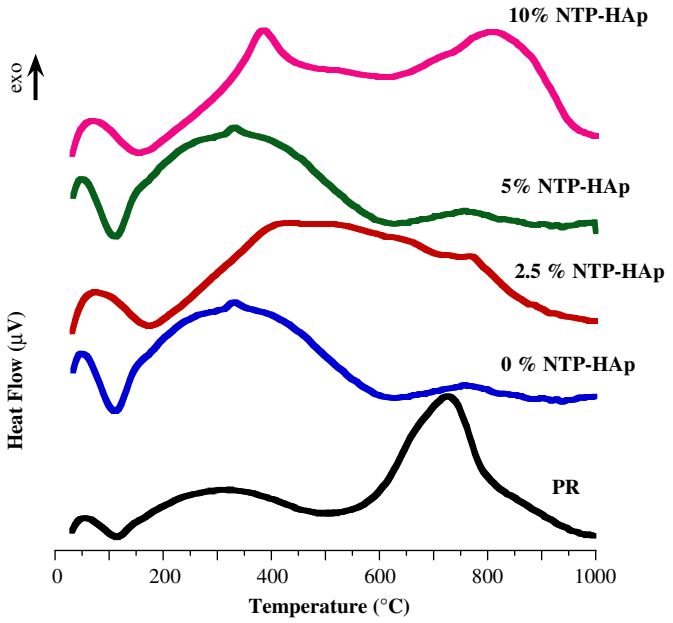

Fig. 7. DTA thermograms of pure and NTP-grafted apatites.

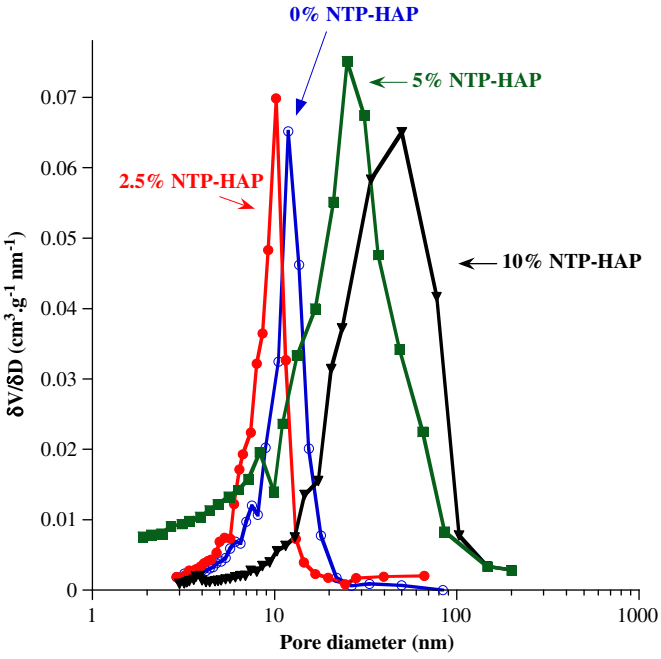

Fig. 9. Pore size distribution from BJH analysis of pure and NTP-grafted apatites.

vibrational bands appear at 2000, 2300 and 2900 cm^{-1} belonging to the aliphatic C–H, N–C and C–P stretch of NTP in the apatite lattice [30].

In order to obtain further information on the conformation and the bonding nature of phosphonate molecules in the apatite structure, ^{31}P and ^{13}C MAS–NMR measurements were performed.

From ^{31}P MAS–NMR analysis of ungrafted apatite (Fig. 4), a single phosphorus peak is observed at 2.9 ppm versus 85% H_3PO_4 similar to that found in synthetic apatites and bone and teeth [31–33]. This confirms that one crystallographic site is available in the structure as demonstrated in previous works [34–36]. In addition to the sharp resonance at 2.9 ppm, one broad resonance around at 19.6 ppm is observed in grafted apatite characteristic of organic phosphorus in NTP species linked to calcium ions, because they have been either adsorbed onto the apatite surface or incorporated into the apatite phosphate structure. We have shown that NMR can be a helpful adjunct to XRD in ascertaining the state of the material. In the examination of the grafted samples, the XRD results indicate the presence of a single apatite phase but give no indication of any organic material or of the relative amounts. ^{13}C NMR spectroscopy (Fig. 5) has identified the carbon environments associated with the organic matter from NTP molecules at 60 ppm and has shown a small quantity of residual carbonate in an apatitic environment at 160 ppm, especially for the HAp reference. Other experiments are now in progress to identify the structural change with heating treatment of grafted samples and to quantify their distribution between the possible sites in the crystal lattice (Figs. 4 and 5).

3.2. Thermal analyses and stability

The TG curves for the as-received products with and without NTP substrates are presented in Fig. 6. It can be obviously seen that a larger weight loss occurs in the temperature range of 200 to 600 °C, which is attributed to the thermal decomposition of organic substrates in the apatite powders. We can observe that the weight loss of the products increases with the grafted NTP content. Another stage is from 600 to 1000 °C, where a small mass loss was observed, and assigned to the departure of the water during structural transformations [37]. We note that the ungrafted apatite has a higher total mass loss than that produced by the modified apatite with 2.5 wt% NTP. We hypothesize that a major part of the weight loss in the ungrafted material comes from water desorption. It is known that native HAp has a hydrophilic surface and absorbs a large amount of water. The DTA thermograms of the grafted apatites are given in Fig. 7. One endothermic peak is observed at 120 °C, attributable to the desorbed

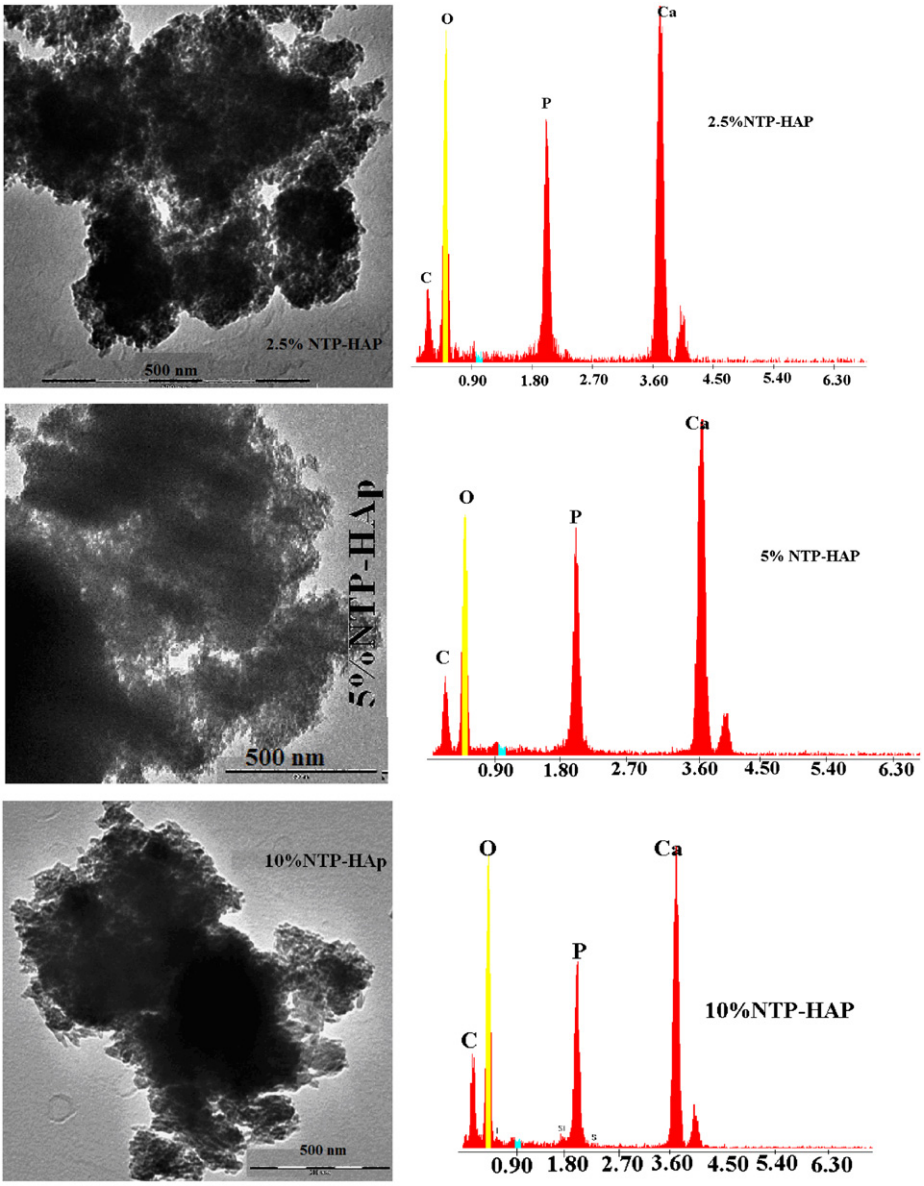

Fig. 10. TEM images of apatite grafted with NTP molecules.

water molecules. The first exothermic peak, beyond 380 °C, corresponds to the combustion of the organic nitrogenous fraction of the sample. Finally, a second exothermic peak at 700 °C is related to the transformation of the apatite phase to β-$Ca_3(PO_4)_2$ following the total combustion of the organic matter.

Chemical analyses of ungrafted and grafted apatites are summarized in Table 1. The synthesis conditions greatly influenced the composition of the grafted HAp powders. With unvarying Ca and P content of the phosphate rock starting material, the added NTP molecules could be differentiated on the basis of the Ca/P molar ratio of the precipitates. For high NTP content, the Ca/P values are close to 1.5, characteristic of β-$Ca_3(PO_4)_2$ detected by XRD for NTP-grafted HAp thermally treated at 800 °C. This confirms the accuracy of the chemical analyses.

3.3. Textural properties

Nitrogen adsorption–desorption on grafted apatite resulted in a type IV isotherm according to Brunauer's classification [38] (Fig. 8). The isotherms exhibit a hysteresis loop which indicates that the grafted samples act as mesoporous materials. As presented in Table 1, the BET specific surface area was 193 $m^2 g^{-1}$ for the 2.5% NTPA-grafted apatite, compared to 150 $m^2 g^{-1}$ for the ungrafted apatite and to 20 $m^2 g^{-1}$ for phosphate rock. Modification by NTP increased the surface area of apatite only at the lowest NTP content; increasing the NTP content resulted in a gradual reduction of surface area at 145 $m^2 g^{-1}$ for 10% NTP content. This is related to the high molecular disorder introduced by the organic molecules into the apatite structure; it was therefore possible that organic matter is located in pores or blocks the pore entrances [30]. Pore size distributions (Fig. 9) indicated the diameter of pores in the functionalized apatite were between 9.5 and 40 nm, including mesopores.

NTP-modified apatite powders were difficult to image by SEM due to the presence of organics. All SEM images mainly showed featureless granular materials, with micron-size platelets being sometimes visible. TEM studies indicated that the materials consist of aggregations of particles; the particles exhibit dimensions well below 100 nm (Fig. 10). Noticeably, 2.5% NTP and 5% NTP showed a rather open structure with individual particles being easy to distinguish, whereas the density of aggregation appeared to increase at 10% NTP. Other particles appeared to consist of barely individual nanoparticles held together by an amorphous, probably organic matrix. The size of the individual NTP–HAp particles in the aggregates ranges from 40 to 90 nm.

4. Conclusions

New organofunctionalized apatites were synthesized from natural phosphate rock by grafting aminotrimethylene phosphonic acid by means of a low-cost process. The introduction of these organic moieties into the apatite lattice most importantly provides an opportunity to control the nanocrystal surface properties that may prove useful in a number of applications. In particular, the introduction of amine groups provides the potential for complexation of metal ions in environmental applications such as the removal of lead from water.

Acknowledgments

The authors would like to thank the Office Chérifien des Phosphates (OCP) and the Center d'Etudes et de Recherches des Phosphates Minéraux (CERPHOS) for their support, UATRS–CNRST–Rabat for chemical analyses, the Martinos Center for Biomedical Imaging at Massachusetts General Hospital and National Institutes of Health grant P41RR14075. S. Saoiabi wishes to acknowledge the Moroccan–American Commission for Educational and Cultural Exchange (MACECE) and the Fulbright Foundation for fellowship support.

References

[1] R.Z. LeGeros, Calcium Phosphates in Oral Biology and Medicine, Karger, Basel, 1991.
[2] J.C. Elliot, Structure and Chemistry of the Apatites and Other Calcium Orthophosphates, Elsevier, Amsterdam, 1994.
[3] M. Vallet-Regi, J.M. Gonzáles-Calbet, Prog. Solid-State Chem 32 (2004) 1–31.
[4] T. Kaludjerovic-Radoicic, S. Raicevic, Chem. Eng. J. 160 (2010) 503–510.
[5] S. El Asri, A. Laghzizil, T. Coradin, A. Saoiabi, A. Alaoui, R. M'hamedi, Colloid Surf. A: Physicochem. Eng. Aspects 362 (2010) 33–38.
[6] H. Bouyarmane, S. El Asri, A. Rami, C. Roux, M.A. Mahly, A. Saoiabi, T. Coradin, A. Laghzizil, J. Hazard. Mater. 181 (2010) 736–741.
[7] M.J. Glimcher, The nature of the mineral phase in bone: Biological and clinical implications, in: L.V. Avioli, S.M. Krane (Eds.), Metabolic Bone Disease and Clinically Related Disorders, Academic Press, New York, 1998, pp. 23–50.
[8] O.G. da Silva, E.C. da Silva Filho, M.G. da Fonseca, L.N.H. Arakaki, J. Colloid Interface Sci. 302 (2006) 485–491.
[9] A. Nakajima, K. Takakuwa, Y. Kameshima, M. Hagiwara, S. Sato, Y. Yamamoto, N. Yoshida, T. Watanabe, K. Okada, J. Photochem. Photobiol. A: Chem 177 (2006) 94–99.
[10] C Hu, J. Guo, J. Qu, X. Hu, Appl. Catal. B: Environ 73 (2007) 345–353.
[11] E. Fujii, M. Ohkubo, K. Tsuru, S. Hayakawa, A. Osaka, K. Kawabata, C. Bonhomme, F. Babonneau, Acta Biomaterialia 2 (2006) 69–74.
[12] H.W. Choi, Lee, K.J. Kim, H.M. Kim, S.C. Lee, J. Colloid Interface Sci. 304 (2006) 277–281.
[13] A. Zieba, G. Sethuraman, F. Perez, G.H. Nancollas, D. Cameron, Langmuir 12 (1996) 2853–2858.
[14] H. Fleisch, Bisphosphonates in Bone Disease: From the Laboratory to the Patient, Academic Press, New York, 2000.
[15] J.A.M. van der Houwen, G. Cressey, B.A. Cressey, E. Valsami-Jones, J. Cryst. Growth 249 (2003) 572–583.
[16] H. Tanaka, A. Yasukawa, K. Kandori, T. Ishikawa, Colloid Surf. A: Physicochem. Eng. Aspects 125 (1997) 53–62.
[17] T. Brendel, A. Engel, C. Russel, J. Mater. Sci.: Mater. Med 3 (1992) 175–179.
[18] L. El Hammari, A. Laghzizil, A. Saoiabi, P. Barboux, M. Meyer, Colloid Surf. A: Physicochem. Eng. Aspects 289 (2006) 84–88.
[19] J.Y. Chane-Ching, A. Lebugle, I. Rousselot, A. Pourpoint, F. Pellé, J. Mater. Chem. 17 (2007) 2904–2913.
[20] L. Wu, F. Willis, P.W. Schindler, J. Colloid Interface Sci. 147 (1991) 178–185.
[21] J. Portier, J.H. Choy, M.A. Subramanian, J. Inorg. Mater. 3 (2001) 581–592.
[22] W. Wengian, J.L. Baptista, Biomaterials 19 (1998) 125–131.
[23] L. Jingbing, Y. Xiaoyue, W. Hao, Z. Mankang, W. Bo, Y. Hui, Ceram. Int. 29 (2003) 629–633.
[24] S. Raynaud, E. Champion, D. Bernache-Assollant, P. Thomas, Biomaterials 23 (2002) 1065–1072.
[25] L. El Hammari, H. Merroun, T. Coradin, A. Laghzizil, P. Barboux, A. Saoiabi, Mater. Chem. Phys. 104 (2007) 448–453.
[26] S. Lazic, S. Zec, N. Miljevic, S. Milonjic, Thermochim. Acta 374 (2001) 13–22.
[27] S. El Asri, A. Laghzizil, A. Alaoui, A. Saoiabi, R. M'Hamdi, K. El Abbassi, A. Hakam, J. Thermal Anal Calorimetry 95 (2009) 15–19.
[28] S. El Asri, A. Laghzizil, A. Saoiabi, A. Alaoui, K. El Abbassi, R. M'hamdi, A. Hakam, T. Coradin, J.Colloid Surf. A: Physicochem. Eng. Aspects 350 (2009) 73–78.
[29] L. El Hammari, H. Marroun, A. Laghzizil, A. Saoiabi, C. Roux, J. Livage, T. Coradin, J. Solid State Chem. 181 (2008) 848–854.
[30] S. Saoiabi, S. El Asri, A. Laghzizil, T. Coradin, K. Lahlil, Mater. Lett. 64 (2010) 2679–2681.
[31] Y. Wu, J.L. Ackerman, E. Strawich, C. Rey, H.M. Kim, M.J. Glimcher, Calcif. Tissue Int. 72 (2003) 610–626.
[32] A.P. Lee, J. Klinowski, J. Archaeol. Sci. 22 (1995) 257–262.
[33] Y. Wu, J.L. Ackerman, H.M. Kim, C. Rey, A. Barroug, M.J. Glimcher, J. Bone Miner. Res. 17 (2002) 472–480.
[34] K. Kandori, A. Fujiwara, A. Yasukawa, T. Ishikawa, Colloid Surf. A: Physicochem. Eng. Aspects 150 (1999) 161.
[35] A. Laghzizil, N. Elherch, A. Bouhaouss, G. Lorent, T. Coradin, J. Livage, Mater. Res. Bull. 36 (2001) 953–962.
[36] A. Laghzizil, P. Barboux, A. Bouhaouss, Solid State Ionics 128 (2000) 177–181.
[37] H. Tanaka, M. Futaoka, R. Hino, J. Colloid Interf. Sci 269 (2004) 358–363.
[38] K.S.W. Sing, D.H. Everett, R.A.W. Haul, L Moscou, R.A. Pierotti, J. Rouquerol, T. Siemieniewska, Pure Appl. Chem. 57 (1985) 603–619.